

A Novel Gallic Acid-Grafted-Lignin Biosorbent for the Selective Removal of Lead Ions from Aqueous Solutions

Xueyan Zhang,^a Can Jin,^{a,*} Yuliang Jiang,^b Guifeng Liu,^a Guomin Wu,^a and Zhenwu Kong^{a,*}

The low content of phenolic groups limits the application of lignin-based materials as biosorbents for the removal of metal ions. In this work, a novel gallic acid-grafted-lignin (GAL, 4.43 mmol/g hydroxyl group) biosorbent was designed by introducing gallic acid moieties to replace the hydroxyl groups of lignin. These grafted polyphenolic groups provide additional sites for the adsorption of metal ions. The structure of GAL was characterized by FT-IR, ³¹P NMR, and ¹³C NMR spectroscopy. The adsorption properties of GAL for Pb(II) ions were investigated under batch conditions. Kinetic and isothermal adsorption processes could be well-described by the pseudo-second order kinetic model and Langmuir isothermal model, respectively. The grafting of polyphenolic groups onto lignin increased the maximum adsorption capacity of the adsorbent for Pb(II) (119.1 mg/g). The adsorption thermodynamics indicated that the adsorption process was endothermic and spontaneous. In addition, GAL could selectively adsorb Pb(II) with a selectivity coefficient (*k*) at 1.89 in the presence of coexisting metal ions from aqueous solution. The high adsorption capacity and selectivity for Pb(II) by GAL, together with its environmental compatibility, enable this material to act as a promising biosorbent for removing heavy metal ions from polluted water.

Keywords: Lignin; Gallic acid; Lead adsorption; Selective adsorption

Contact information: a: Institute of Chemical Industry of Forest Products, Chinese Academy of Forestry; National Engineering Laboratory for Biomass Chemical Utilization; Key Laboratory of Biomass Energy and Material of Jiangsu Province, Nanjing 210042, China; b: School of Chemistry and Materials Science, Nanjing Normal University, Nanjing 210097, China;

* Corresponding authors: (C. Jin) envis@163.com, (Z. Kong) kongzwlhs@163.com

INTRODUCTION

Water pollution caused by heavy metal ions has been a severe threat to the environment (Liu *et al.* 2016). Lead, one of the most toxic metal ions, tends to accumulate in living organisms and cause serious damage, such as memory loss, irritability, anemia, and mental retardation (Zhang *et al.* 2011). Pb(II) ions can be easily encountered in the environment because of its previous and present usage in pigments, gasoline, batteries, *etc.* (Satapathy *et al.* 2012). Thus, the presence of Pb(II) ions has raised concerns and initiated searches for treatments in its effective elimination from aqueous solutions (Gupta *et al.* 2011). Many treatment methods such as chemical precipitation, oxidation/reduction, membrane filtration, adsorption, ion-exchange and reverse osmosis had been applied in the removal of Pb(II) ions from wastewater (Wang *et al.* 2010; Luo *et al.* 2013; Gupta *et al.* 2012); however, few of these methods are favored because of their high costs and low efficiencies. Therefore, high-performance and environmentally compatible adsorbents regarding their structural design, synthesis, and specific properties are needed. Biomass materials, including cellulose, lignin, chitosan, and agricultural wastes, are currently

preferred to develop new low-cost biosorbents because of their natural abundance, low cost, biocompatibility, and biodegradability (Luo *et al.* 2016).

Lignin, the second most abundant biomass only after cellulose, has a branched structure containing phenolic, carbonyl, and ether groups which can adsorb metal ions as active sites (*e.g.*, Hg(II), Cr(VI), Cu(II), and Pb(II)); however, raw lignin usually has low content of those functional groups, which results in the low adsorption capacity for metal ions (Li *et al.* 2015a, Gregorova and Sedlarik 2015); this factor significantly restricts the large-scale usage of lignin adsorbents. Therefore, detailed studies are required to obtain a quantitative and mechanistic understanding of the role that active sites play in the adsorption for metal ions by lignin adsorbents.

In this study, gallic acid-grafted-lignin (GAL) adsorbent was synthesized *via* an esterification reaction with a protecting group strategy to improve the cation adsorption capacity of the lignin. Gallic acid (GA), a naturally polyphenolic compound derived from plants, is known to bind strongly to surfaces through covalent and non-covalent interactions with metal ions (Vasic *et al.* 2012), which inspires our interests in this compound as a lignin modifying agent. Although there have been few reports on the phenolation process for lignin-based thermoset polymers (Podschn *et al.* 2015), the incorporation of natural polyphenolic GA onto lignin with improving adsorption capacity for heavy metal ions is unprecedented. We anticipate that the grafting of GA moieties, with its three phenolic groups, onto lignin will enhance the lignin's cation adsorption capacity. The obtained GAL was characterized, and its adsorption properties for Pb(II) ions were explored. The adsorption kinetics, isotherms, and thermodynamics were systematically studied. Furthermore, the adsorption selectivity of GAL for Pb(II) ions in solution by was also investigated.

EXPERIMENTAL

Materials

Industrial bamboo lignin ($M_w = 2200$ g/mol; elemental analysis: 60.92% C, 5.47% H, and 0.75% N) was obtained using acetic acid treatment from Kong Long Paint Co. (Beijing, China). Gallic acid (GA, 99% purity) was purchased from Aladdin Industrial Corp. (Shanghai, China). Analytical grade tetrahydrofuran (THF), dichloromethane (DCM), toluene, triethylamine (TEA), lead nitrate, copper nitrate, cadmium nitrate, nickel nitrate, zinc nitrate, sodium hydroxide (NaOH), acetic anhydride, thionyl chloride, and sodium acetate were purchased from Sinopharm Chemical Reagent Co. Ltd. (Shanghai, China).

Preparation of GAL

Gallic acid-grafted-lignin was prepared following the synthesis route shown in Fig. 1. Acetyl-protected GA (3,4,5-triacetoxybenzoic acid, 90% yield) was prepared and purified according to the method of Ye *et al.* (2010). Next, the acetyl-protected GA (5.0 g, 16.9 mmol) was dissolved in anhydrous DCM (60 mL), and excess thionyl chloride (15 mL, 206 mmol) was added to the solution with stirring. The solution was heated with reflux at 55 °C for 90 min; afterwards, the DCM and excess thionyl chloride were carefully removed on a rotary evaporator; the crude product was washed with dried toluene (30 mL) to afford 3,4,5-triacetoxybenzoic chloride as a pale yellow crystalline product (5.1 g, 16.2 mmol, 96% yield).

Excess 3,4,5-triacetoxybenzoic chloride (1.12 g, 3.53 mmol) and bamboo lignin (1.1 g, 2.35 mmol hydroxyl group) were both dissolved in dried THF. After triethylamine (TEA, 1.8 mL) was added to the solution, the mixture was allowed to react at 50 °C for 5 h with stirring. Then, the THF solvent was removed using a rotary evaporator. The crude mixture was washed with deionized water and ethanol, and the washed solids were dried under vacuum to yield the esterified GA-*grafted*-lignin (1.73 g, 91% yield).

The esterified GA-*grafted*-lignin was added to a THF/water (40:5 v/v) solution with sodium acetate. The resulting solution was stirred for 5 h at room temperature for the removal of acetyl protection groups. The crude product was washed with deionized water three times and then dried in vacuum oven at 40 °C for 10 h to yield GA-*grafted*-lignin adsorbent (GAL) as a reddish brown powder.

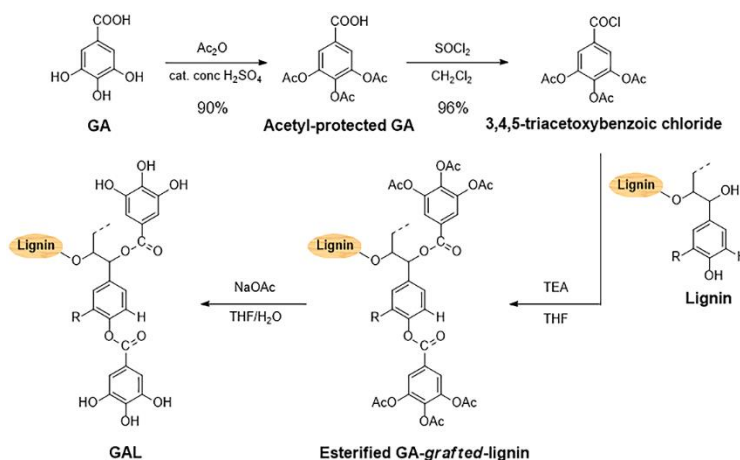


Fig. 1. Synthesis route of gallic acid-*grafted*-lignin (GAL) adsorbent

Characterization

Fourier transform infrared (FT-IR) spectra of samples were recorded in the range of 4000 to 500 cm⁻¹ on a Nicolet iS10 spectrometer (Nicolet Instrument Corp. (Madison, WI, USA)) utilizing KBr pressed pellets. ³¹P NMR spectra of unmodified lignin and GAL were recorded on a Brüker 500 MHz NMR spectrometer (Brüker BioSpin (Rheinstetten, Germany)) according to the method of Xin *et al.* (2014) using 2-chloro-4,4,5,5-tetramethyl-1,2,3-dioxaphospholane (TMDP) as the phosphitylating reagent. ¹³C NMR spectra were recorded on a 500 MHz Brüker spectrometer (Brüker BioSpin, Rheinstetten, Germany).

Batch adsorption

Batch adsorption experiments were carried out by mixing 20 mg of GAL and 10 mL of aqueous Pb(II) solution. The mixtures were placed into flat-bottom flasks and stirred at 200 rpm with a magnetic mixing bar to guarantee good dispersion. The flasks were placed in a water bath at the desired temperature ranging from 25 to 45 °C for a suitable contact time (*e.g.*, 180 min except for kinetic adsorption experiments) to allow for complete equilibration. The pH of the solutions, which ranged from 3.0 to 6.0, was adjusted using either 0.1 M HCl or 0.1 M NaOH solutions. The effect of initial concentration on adsorption was determined with Pb(II) solutions of 25 to 500 mg/mL at pH 6. Kinetic adsorption experiments were conducted with Pb(II) concentrations of 200 mg/L (pH 6) using a GAL adsorbent dosage of 20 mg/10 mL. At predetermined time intervals, the sample solutions were pipetted from the flat-bottom flasks and filtered immediately through membranes

(0.22 μm pore-size). The concentrations of Pb(II) solution were determined by inductive coupled plasma optical emission spectrometry (ICP-OES, optima 200 DV, Perkin-Elmer (Waltham, MA, USA) or atomic absorption spectroscopy (AAS, PEAA-300, Perkin-Elmer (Waltham, MA, USA)). The adsorption capacity (Q_e) was calculated by Eq. 1,

$$Q_e = \frac{(C_0 - C_e)}{m} V \quad (1)$$

where C_0 (mg/L) and C_e (mg/L) are the initial and equilibrium concentrations of Pb(II) in solution, respectively, V (L) is the volume of the solution, and m (mg) is the mass of GAL dosage.

Selectivity adsorption

An adsorbent dosage of 20 mg/10 mL (lignin or GAL) was added to a solution containing Pb(II), Cu(II), Cd(II), Ni(II), and/or Zn(II) ions; the initial concentration of each species was 200 mg/L (at pH 6.0). The adsorption time was 180 min at 25 °C. The selectivity coefficient, k , was calculated according to Eq. 2,

$$k = \frac{Q_x}{Q'} \quad (2)$$

where Q_x (mg/g) is the adsorption capacity of the X cation in the mixed solution, and Q' (mg/g) is the total adsorption capacity of the other metal ions except X cation in the mixed solution.

RESULTS AND DISCUSSION

Synthesis and Characterization

Before grafting GA moieties onto the surface of lignin, it is necessary to protect the polyphenolic groups of GA to prevent them from undergoing self-condensation and/or unproductive side reactions. 3,4,5-Triacetoxybenzoic acid (acetyl-protected GA) was synthesized from GA, which was subsequently converted to the highly reactive 3,4,5-triacetoxybenzoic chloride (at 96% yield).

Esterified GA-grafted-lignin was synthesized in dried THF solution using TEA as a catalyst and an acid-binding agent; afterwards, the acetyl protecting groups were removed to yield GAL, as detailed in Fig. 1.

The FT-IR spectra of the unmodified lignin and the GAL are shown in Fig. 2. The lignin spectra exhibits a strong and broad band around 3391 cm^{-1} , which is characteristic of hydroxyl group. The peak at 2931 cm^{-1} is associated with C-H stretching of methyl or methylene groups. Two strong signals at 1222 and 1118 cm^{-1} are attributed to guaiacyl (G) and syringyl (S) lignin units, respectively, which indicated that the lignin extracted from bamboo is a GS-type lignin (She *et al.* 2010).

Compared to the unmodified lignin, the GAL has higher absorption peaks at 1719 and 1187 cm^{-1} , which are attributed to the C=O and C-O stretching of ester groups. This observation suggested that the modified lignin contained more carbonyl moieties (Laurichesse *et al.* 2014).

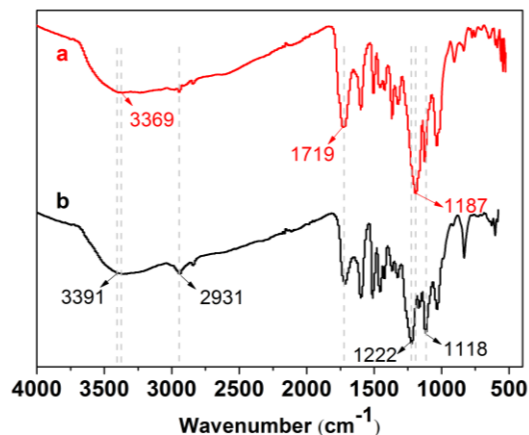


Fig. 2. FT-IR spectra of (a) GAL and (b) unmodified lignin

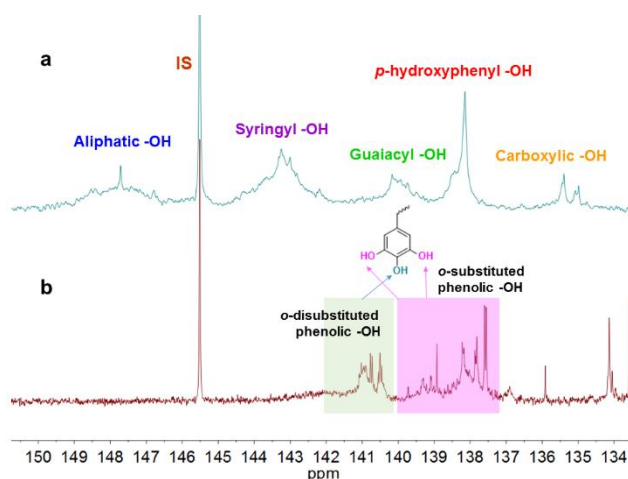


Fig. 3. Quantitative ^{31}P NMR spectra of (a) unmodified lignin and (b) GAL

^{31}P NMR spectra (Fig. 3) were recorded to quantify the different types of free hydroxyl groups (*i.e.*, aliphatic and phenolic) contained in the unmodified lignin and GAL. The amount of aliphatic hydroxyl groups in lignin was determined to be 0.56 mmol/g. In addition to the aliphatic hydroxyl groups, the total content of phenolic hydroxyl groups which included syringyl (S), guaiacyl (G), and *para*-hydroxyphenyl (H) units was 1.58 mmol/g. As for the GAL, the esterification process reduced the aliphatic hydroxyl content (150 to 145.5 ppm), whereas the addition of GA units increased the phenolic hydroxyl content (144.7 to 136.6 ppm), which was expected. Additionally, the peaks for S-type (around 142.7 ppm), G-type (140.0 to 139.0 ppm), and H-type (139.5 to 137.3 ppm) phenolic hydroxyl groups disappeared and were replaced with *ortho*-disubstituted (142.0 to 140.4 ppm) and *ortho*-substituted (140.3 to 137.6 ppm) phenolic hydroxyl groups from GA resource (Melone *et al.* 2013). The grafted GA moieties of GAL increased the phenolic hydroxyl content to 4.43 mmol/g as compared to 2.14 mmol/g for unmodified lignin; the grafting increased the molecular weight (M_w) from 2200 g/mol for the unmodified lignin to 2996 g/mol for the GAL. The M_w of the GAL was calculated according to a molar mass balance (Eq. 3),

$$\frac{m + \frac{m \times 2.14 \times 169.12}{1000}}{M_w} = \frac{m}{2200} \quad (3)$$

where m (g) is the mass of unmodified lignin, 2.14 mmol/g is the total hydroxyl groups in the unmodified lignin, 169.1 g/mol is the molecular weight of GA, and M_w (g/mol) is the molecular weight of GAL.

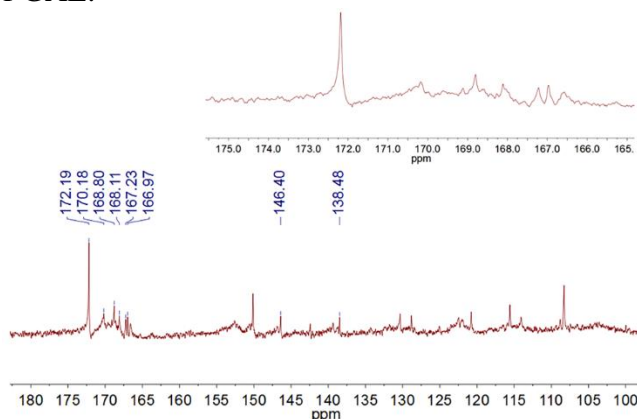


Fig. 4. ^{13}C NMR (DMSO- d_6) spectra of GAL with expanded ester region (175 to 165 ppm)

All functional groups of lignin can be identified in the ^{13}C NMR spectra according to the literature review of peak assignments by Balakshin and Capanema (2015). The spectra ranging from 172 to 165 ppm typically contains signals for ester carbons. Within this region, the GAL spectra had peaks clearly indicating the existence of ester groups (Fig. 4). Analogous to the ^{31}P NMR spectral analysis, there were good correlations of certain ^{13}C NMR resonances in the recorded spectra (not shown), which provided supporting evidence for GA grafting in the GAL.

Effect of Adsorption pH

The pH of the solution plays a key role in the adsorption of heavy metal ions. The effect of pH on Pb(II) adsorption by GAL was studied over the range of 3.0 to 6.0 at 25 °C. The GAL adsorbent dosage was set to 20 mg/10 mL, and a contact time of 180 min was employed. As shown in Fig. 5, the solution's pH greatly influenced the adsorption capacity of GAL for Pb(II) ions.

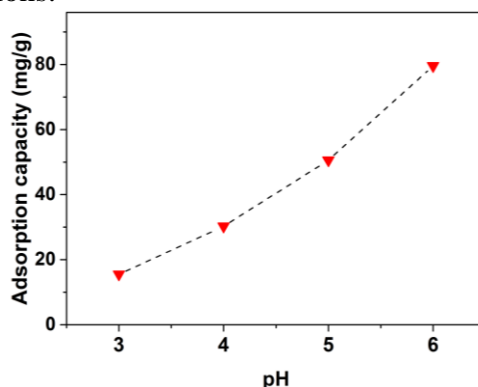


Fig. 5. Effect of solution pH on the adsorption of Pb(II) by GAL

The low adsorption capacities at lower pH were attributed to the competitive adsorption of protons and Pb(II) on the surface of GAL. As pH value increased, the weakened electrostatic repulsive forces by protons greatly improved the Pb(II) adsorption. The adsorption capacity, Q_e , was low at 15.5 mg/g at pH 3.0; it increased five-fold to 80.1 mg/g at pH 6.0. Moreover, the insoluble hydroxide $\text{Pb}(\text{OH})_2$ could be formed at a higher

pH (Akbulut *et al.* 2016). Hence, to avoid the precipitation of Pb(II) as Pb(OH)₂, the solution pH was limited at the upper value of 6.0 for future adsorption experiments.

Effect of Contact Time and Adsorption Kinetics

The effect of contact time on adsorption was investigated. The adsorption capacity (Q_e) of GAL for Pb(II) was examined for different time intervals up to 240 min with a C_0 value of 200 mg/L, pH 6.0, adsorbent dosage of 20 mg/10 mL, and temperature of 35 °C. The Q_e value increased rapidly during the 60 min time interval; afterwards, Q_e rose more slowly to the saturation limit and reached equilibrium at approximately 120 min (Fig. 6a).

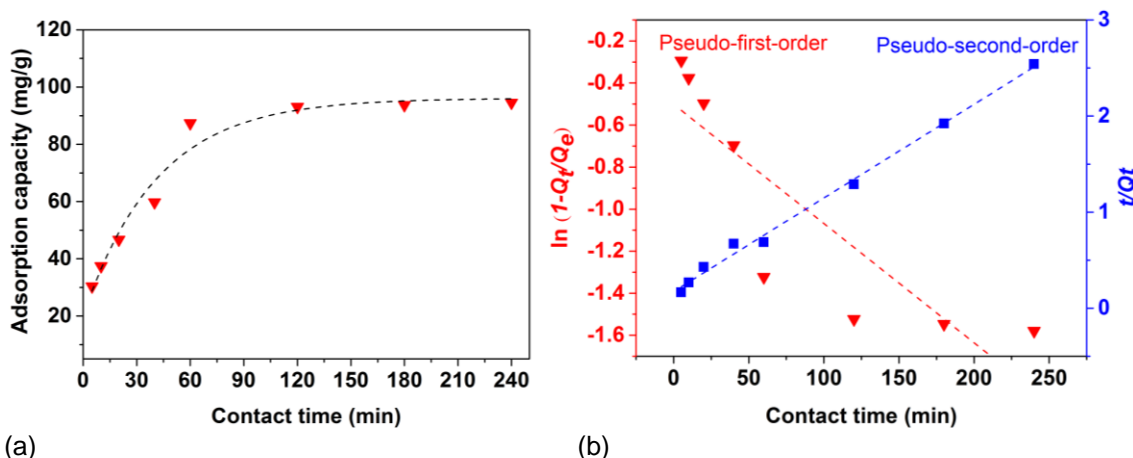


Fig. 6. (a) Effect of contact time on the adsorption of Pb(II) by GAL, and (b) fitted results for pseudo-first-order and pseudo-second-order kinetic models

Pseudo-first-order and pseudo-second-order models were utilized to evaluate the experimental kinetic data (Ge *et al.* 2014b), which are given in Eq. 4 and Eq. 5, respectively,

$$\log(Q_e - Q_t) = \log Q_e - \left(\frac{k_1 t}{2.303}\right) \log(1 - Q_t/Q_e) = -k_1 t \quad (4)$$

$$\frac{t}{Q_t} = \frac{1}{k_2 Q_e^2} + \frac{t}{Q_e} \quad (5)$$

where k_1 (min^{-1}) is the pseudo-first-order rate constant, k_2 ($\text{g mg}^{-1} \cdot \text{min}^{-1}$) is the pseudo-second-order kinetic rate constant, and Q_e and Q_t (mg/g) are the adsorption capacities of GAL for Pb(II) at equilibrium and at contact time t (min), respectively. The fitted results are shown in Fig. 6b, and the parameter values are listed in Table 1. The coefficient of determination (R^2) of the pseudo-second-order model was 0.9931, which was much higher than that of the pseudo-first-order model ($R^2 = 0.7223$), indicating a better fitting for the adsorption kinetic data. Moreover, the calculated Q_e for pseudo-second-order kinetic model (101.6 mg/g) was found to be closer to the experimental data (94.5 mg/g).

Table 1. Kinetic Model Parameter Values for Pb(II) Adsorption by GAL

Pseudo-first-order model			Pseudo-second-order model		
K_1 (min^{-1})	R^2	Q_e (mg/g)	K_2 [$\text{g}/(\text{mg}\cdot\text{min})$]	R^2	Q_e (mg/g)
0.0205	0.7223	82.25	5.446×10^{-4}	0.9931	101.61

Effect of Initial Lead Concentration and Adsorption Isotherm

The effect of initial Pb(II) concentration on GAL adsorption kinetics was investigated. Experiments were conducted at C_0 ranging from 25 to 500 mg/L, pH 6, adsorbent dosage of 20 mg/10 mL, 180 min adsorption time, and 25 °C. The Q_e value increased sharply at low concentration (Fig. 7a), then plateaued to a maximum Q_e of 113.7 mg/g. This observation can be explained that there are fewer active sites on the surface of GAL that are available for additional Pb(II) adsorption at the higher initial ion concentrations.

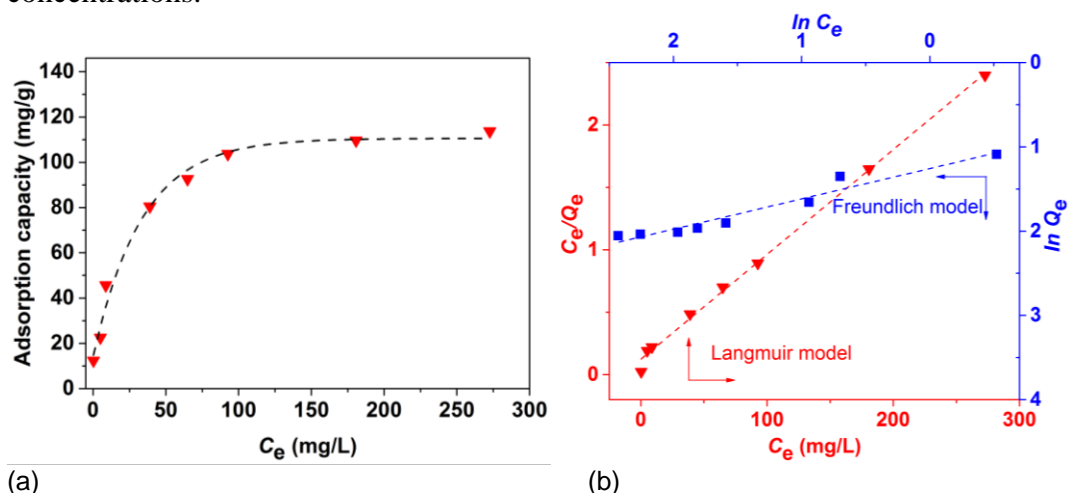


Fig. 7. (a) Effect of initial Pb(II) concentration on Pb(II) adsorption by GAL, and (b) fitted results of adsorption isotherms by Langmuir and Freundlich models

Langmuir and Freundlich isotherm models were applied to analyze the experimental data. The Langmuir adsorption isotherm model (Eq. 6) assumes that all adsorption sites are equivalent and that there is a monolayer coverage of the adsorbent on the surface. The Freundlich isotherm model (Eq. 7) supposes that the adsorption process occurs heterogeneously on the surface with multilayer adsorption. The models are, respectively,

$$\frac{C_e}{Q_e} = \frac{1}{k_L Q_{max}} + \frac{C_e}{Q_{max}} \quad (6)$$

$$\ln Q_e = \ln K_F + \ln C_e / n \quad (7)$$

where Q_e (mg/g) is adsorption capacity of GAL for Pb(II) at equilibrium, C_e (mg/L) is the metal ion concentration in solution at equilibrium, K_L is the Langmuir equilibrium constant, and Q_{max} is the maximum adsorption capacity (mg/g). Thus, a plot of C_e/Q_e versus C_e should yield a straight line with a slope of $1/Q_{max}$ and a y-intercept of $1/K_L Q_{max}$. In Eq. 7, K_F is the Freundlich constant and n is a constant related to the site heterogeneities of the adsorbent surface.

Table 2. Isotherm Parameters of Langmuir and Freundlich Models

Langmuir model			Freundlich model		
K_L (L/mg)	R^2	Q_e (mg/g)	K_F	R^2	n
0.0682	0.9965	119.1	17.63	0.9448	2.6148

The calculated parameters for the Langmuir and Freundlich models from the nonlinear regressions of the experimental data are shown in Fig. 7b and Table 2. The adsorption isotherm behavior could be well represented by the Langmuir adsorption model ($R^2 = 0.9965$). The GAL had a monolayer adsorption capacity value ($Q_{max} = 119.1$ mg/g), which was in good agreement with the experimentally measured saturation value ($Q_e = 113.7$ mg/g). The Freundlich model had a lower coefficient of determination ($R^2 = 0.9448$) versus the Langmuir model, which indicated that it was not able to describe the relationship between the amount of adsorbed Pb(II) and its equilibrium concentration in solution. These observations indicated that the GAL surface was homogeneous and that the adsorption process occurred *via* monolayer adsorption (Wang *et al.* 2015). The adsorption capacity obtained from this study was compared to various reported adsorbents (Table 3). It was clear that the GAL had a higher adsorption capacity for Pb(II) than most other adsorbents. Moreover, GAL has the advantage of being a 100% biomass-based biosorbent that is efficient at Pb(II) removal; there are other biosorbents listed in Table 3 that exhibit higher adsorption capacities than GAL.

Table 3. Adsorption Capacities for Various Adsorbents for Pb(II) Ions

Adsorbent	Adsorption capacity (Q_{max} , mg/g)	Reference
Porous lignin-based sphere (PLS)	31.8	Li <i>et al.</i> 2015a
Lignin xanthate resin (LXR)	64.9	Li <i>et al.</i> 2015b
Amine functionalized lignin (AML)	69.4	Ge <i>et al.</i> 2015
Amino and sulfonic-functionalized lignin (ASL)	67.59	Ge <i>et al.</i> 2014a
Lignin	89.51	Guo <i>et al.</i> 2008
Lignin from beech wood	8.2	Demirbas 2004
Lignin from poplar wood	9.0	Demirbas 2004
Lignin grafted carbon nanotubes (L-CNTs)	251	Li <i>et al.</i> 2017
Citric acid modified wood	82.64	Low <i>et al.</i> 2004
Peanut husk powder (PHP)	27.03	Abdelfattah <i>et al.</i> 2016
Carbon nanotube sheets	117.65	Tofighy <i>et al.</i> 2011
Poly(ethyleneimine)/Silica gel	82.64	Ghoul <i>et al.</i> 2003
GAL	119.1	This study

Effect of Temperature and Adsorption Thermodynamics

The effect of temperature on GAL adsorption was investigated at temperatures of 15, 25, 35, 45, and 55 °C. Experiments were conducted at: C_0 of 100, 200, and 500 mg/L; pH 6; adsorbent dosage of 20 mg/10 mL; and 180 min adsorption time. The results are

shown in Fig. 8a. It was observed that the adsorption capacities of GAL for Pb(II) increased as the adsorption temperature increased for all C_0 values examined. High adsorption temperatures decrease the viscosity of the aqueous solution, but also increase the rate of adsorbent molecules passing through the external boundary layer and the internal pores of the adsorbent particles (Chowdhury *et al.* 2011). Hence, the enhanced adsorption capacity occurred as the frequency of collisions between GAL and Pb(II) increased with higher adsorption temperatures.

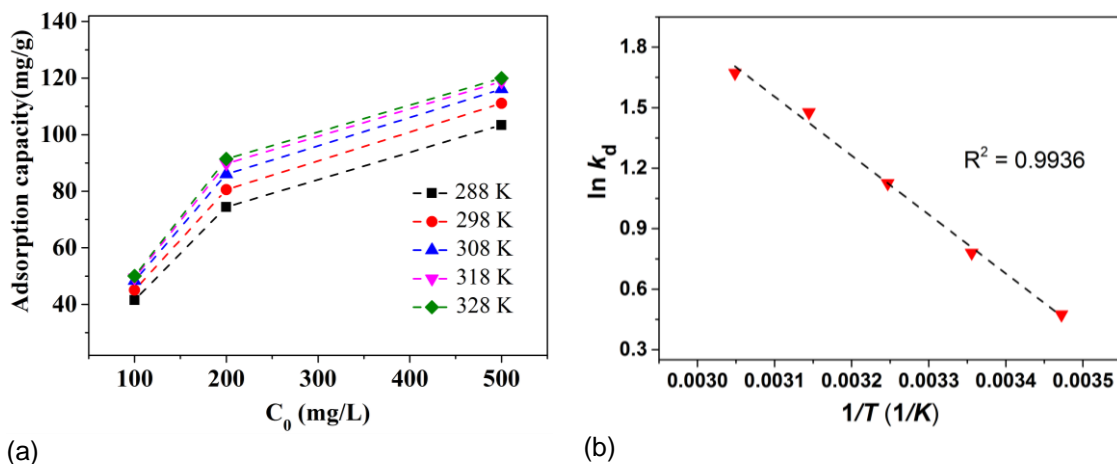


Fig. 8. (a) Effect of different temperatures on the adsorption of Pb(II) by GAL at different initial concentrations, and (b) plot of $\ln(k_d)$ versus $1/T$ for the adsorption of Pb(II) by GAL ($C_0 = 200$ mg/L).

A thermodynamic analysis was performed to understand the Pb(II) adsorption process at different temperatures. The changes in standard Gibbs free energy (ΔG° (kJ mol^{-1})), enthalpy (ΔH° (kJ mol^{-1})) and entropy (ΔS° ($\text{J mol}^{-1} \text{K}^{-1}$)) were calculated according to following equations (Liu *et al.* 2015),

$$\Delta G^\circ = -RT \ln(k_d) \quad (8)$$

$$\ln k_d = -\frac{\Delta H^\circ}{RT} + \frac{\Delta S^\circ}{R} \quad (9)$$

$$k_d = \frac{Q_e}{C_e} \quad (10)$$

where R is the universal gas constant ($8.314 \text{ J mol}^{-1} \text{K}^{-1}$), T (K) is the absolute temperature, and k_d is the thermodynamic equilibrium coefficient. The results are listed in Table 4. Figure 8b shows that the thermodynamic equilibrium coefficient, k_d , increased with increasing temperature, which confirmed that the adsorption process was endothermic.

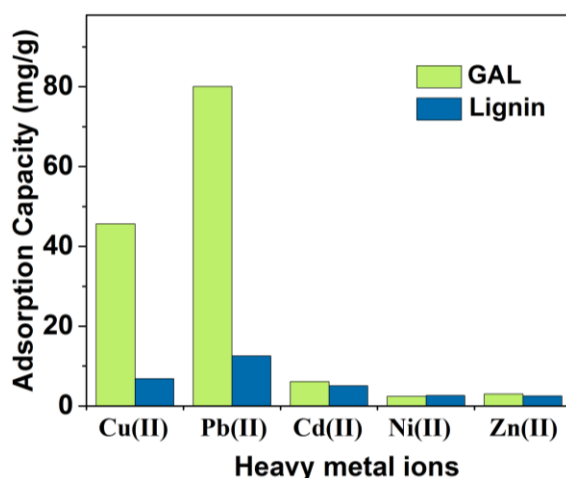
As shown in Table 4, ΔG° decreased as adsorption temperature increased, which indicated the spontaneity of adsorption process (Hou *et al.* 2015). The positive ΔH° value ($24.32 \text{ kJ mol}^{-1}$) confirmed that adsorption process was endothermic and was energetically stable. The positive ΔS° value ($88.32 \text{ J mol}^{-1} \text{K}^{-1}$) revealed the randomness at solid/solution interface increased during the GAL adsorption of Pb(II) ions.

Table 4. Thermodynamic Parameters of GAL Adsorption of Pb(II) Ions

T (K)	ΔG° (kJ mol ⁻¹)	ΔH° (kJ mol ⁻¹)	ΔS° (J mol ⁻¹ K ⁻¹)
288	-1.14	24.32	88.32
298	-1.81		
308	-2.88		
318	-3.90		
328	-4.56		

Adsorption Selectivity

Comparisons of unmodified lignin and GAL for adsorbing various metal ions was investigated. Experiments were conducted with solutions containing Pb(II), Cu(II), Cd(II), Ni(II), and Zn(II) ions individually. As shown in Fig. 9, the adsorption capacities of GAL for metal ions was enhanced when compared to those of the unmodified lignin; this observation could be attributed to the grafting of polyphenolic groups as adsorption sites for GAL. Additionally, GAL was found to have a much higher adsorption capacity value for Pb(II) ions over the other divalent metal ions with an order of Pb(II) > Cu(II) \gg Cd(II) > Ni(II) \approx Zn(II).

**Fig. 9.** Comparisons of the adsorption of different divalent metal ions by unmodified lignin and GAL

Competitive adsorption experiments were designed to further study the adsorption behaviors of Pb(II) by unmodified lignin and GAL with aqueous solutions containing Cu(II), Cd(II), Ni(II), and Zn(II) ions together. According to Eq. 2, the values of the selectivity coefficients, k , of lignin and GAL adsorbents for various metal ions were calculated and listed in Table 5. GAL had the highest k value for Pb(II) (1.89) versus that of the unmodified lignin (0.75) (Zhu *et al.* 2016). In addition, the k value for Pb(II) was much higher than the k values for Cu(II), Cd(II), Ni(II) and Zn(II) ions. Such observation suggested that GAL could selectively adsorb Pb(II) from a solution containing other divalent metal ions. This phenomenon might be explained that Pb(II) is an oxyphilic element metal ion and acts as a soft acid that preferentially adsorbs onto active phenolic sites, which acts as a soft base according to HSAB theory (Li *et al.* 2015c).

Table 5. Selectivity Parameters of Unmodified Lignin and GAL Adsorbents for Metal Ions

Adsorbent	Selectivity coefficient k				
	k (Pb)	k (Cu)	k (Cd)	k (Zn)	k (Ni)
Lignin	0.75	0.41	0.39	-	-
GAL	1.89	0.44	0.04	-	-

CONCLUSIONS

1. A novel gallic acid-*grafted*-lignin (GAL) biosorbent, containing polyphenolic moieties instead of hydroxyl lignin groups, was prepared and thoroughly characterized by FT-IR, ^{31}P NMR, and ^{13}C NMR analyses.
2. The effects of adsorption conditions such as pH, contact time, initial Pb(II) concentration and temperature on the adsorption capacity of GAL for Pb(II) were systematically investigated.
3. The adsorption kinetics could be well-fitted by a pseudo-second-order model. The adsorption isotherms were well-described using the Langmuir model. GAL showed a higher adsorption capacity ($Q_{\text{max}} = 119.1 \text{ mg/g}$) for Pb(II) ions than that of many reported adsorbents. The thermodynamic data analysis indicated that the Pb(II) adsorption process was spontaneous and endothermic.
4. Whole biomass-based GAL was capable of selectively adsorbing Pb(II) from an aqueous solution containing Cu(II), Cd(II), Ni(II) and Zn(II) ions.
5. GAL, an environmentally compatible and biodegradable material made from natural products, exhibits high potential for the removal of heavy metal ions from contaminated water.

ACKNOWLEDGMENTS

This work was supported by the National Science & Technology Pillar Program during the Twelfth Five-Year Plan Period (No. 2015BAD14B06).

REFERENCES CITED

- Abdelfattah, I., Ismail, A. A., Sayed, F. A., Almedolab, A., and Aboelghait, K. M. (2016). "Biosorption of heavy metals ions in real industrial wastewater using peanut husk as efficient and cost effective adsorbent," *Environ. Nanotechnol. Monit. Manag.* 6, 176-183. DOI: 10.1016/j.enmm.2016.10.007
- Akbulut, H., Yamada, S., and Endo, T. (2016). "Preparation of a zwitterionic polymer based on l-cysteine for recovery application of precious metals," *RSC Adv.* 6(110), 108689-108696. DOI: 10.1039/c6ra23359g
- Balakshin, M. Y., and Capanema, E. A. (2015). "Comprehensive structural analysis of biorefinery lignins with a quantitative ^{13}C NMR approach," *RSC Adv.* 5(106), 87187-

87199. DOI: 10.1039/c5ra16649g
- Chowdhury, S., Mishra, R., Saha, P., and Kushwaha, P. (2011). "Adsorption thermodynamics, kinetics and isosteric heat of adsorption of malachite green onto chemically modified rice husk," *Desalination* 265(1-3), 159-168. DOI: 10.1016/j.desal.2010.07.047
- Demirbas, A. (2004). "Adsorption of lead and cadmium ions in aqueous solutions onto modified lignin from alkali glycerol delignification," *J. Hazard. Mater.* 109(1-3), 221-226. DOI: 10.1016/j.jhazmat.2004.04.002
- Ge, Y., Li, Z., Kong, Y., Song, Q., and Wang, K. (2014a). "Heavy metal ions retention by bi-functionalized lignin: Synthesis, applications, and adsorption mechanisms," *J. Ind. Eng. Chem.* 20(6), 4429-4436. DOI: 10.1016/j.jiec.2014.02.011
- Ge, Y., Xiao, D., Li, Z., and Cui, X. (2014b). "Dithiocarbamate functionalized lignin for efficient removal of metallic ions and the usage of the metal-loaded bio-sorbents as potential free radical scavengers," *J. Mater. Chem. A* 2(7), 2136-2145. DOI: 10.1039/c3ta14333c
- Ge, Y., Song, Q., and Li, Z. (2015). "A Mannich base biosorbent derived from alkaline lignin for lead removal from aqueous solution," *J. Ind. Eng. Chem.* 23, 228-234. DOI: 10.1016/j.jiec.2014.08.021
- Ghoul, M., Bacquet, M., and Morcellet, M. (2003). "Uptake of heavy metals from synthetic aqueous solution using modified PEI-silica gels," *Water Res.* 37(4), 729-734. DOI: 10.1016/S0043-1354(02)00410-4
- Gregorova, A., and Sedlarik, V. (2015). "Characterization of structural and physical properties of dichloromethane- and methanol-fractionated kraft lignin and its adsorption capacity of Cu (II) and Ni (II) ions," *Desalin. Water Treat.* 57(23), 10655-10663. DOI: 10.1080/19443994.2015.1036364
- Guo, X., Zhang, S., and Shan, X.-Q. (2008). "Adsorption of metal ions on lignin," *J. Hazard. Mater.* 151(1), 134-142. DOI: 10.1016/j.jhazmat.2007.05.065
- Gupta, V. K., Agarwal, S., and Saleh, T. A. (2011). "Synthesis and characterization of alumina-coated carbon nanotubes and their application for lead removal," *J. Hazard. Mater.* 185(1), 17-23. DOI: 10.1016/j.jhazmat.2010.08.053
- Gupta, V. K., Ali, I., Saleh, T. A., Nayak, A., and Agarwal, S. (2012). "Chemical treatment technologies for waste-water recycling – An overview," *RSC Adv.* 2(16), 6380-6388. DOI: 10.1039/c2ra20340e
- Hou, H., Yu, D. and Hu, G. (2015). "Preparation and properties of ion-imprinted hollow particles for the selective adsorption of silver ions," *Langmuir* 31(4), 1376-1384. DOI: 10.1021/la5032784
- Laurichesse, S., Huillet, C., and Averous, L. (2014). "Original polyols based on organosolv lignin and fatty acids: New bio-based building blocks for segmented polyurethane synthesis," *Green Chem.* 16(8), 3958-3970. DOI: 10.1039/c4gc00596a
- Li, Z., Ge, Y., and Wan, L. (2015a). "Fabrication of a green porous lignin-based sphere for the removal of lead ions from aqueous media," *J. Hazard. Mater.* 285, 77-83. DOI: 10.1016/j.jhazmat.2014.11.033
- Li, Z., Kong, Y., and Ge, Y. (2015b). "Synthesis of porous lignin xanthate resin for Pb²⁺ removal from aqueous solution," *Chem. Eng. J.* 270, 229-234. DOI: 10.1016/j.cej.2015.01.123
- Li, Z., Xiao, D., Ge, Y., and Koehler, S. (2015c). "Surface-functionalized porous lignin for fast and efficient lead removal from aqueous solution," *ACS Appl. Mater. Interf.* 7(27), 15000-15009. DOI: 10.1021/acsami.5b03994

- Li, Z., Chen, J., and Ge, Y. (2017). "Removal of lead ion and oil droplet from aqueous solution by lignin-grafted carbon nanotubes," *Chem. Eng. J.* 308, 809-817. DOI: 10.1016/j.cej.2016.09.126
- Liu, C. H., Chuang, Y. H., Chen, T. Y., Tian, Y., Li, H., Wang, M. K., and Zhang, W. (2015). "Mechanism of arsenic adsorption on magnetite nanoparticles from water: Thermodynamic and spectroscopic studies," *Environ. Sci. Technol.* 49(13), 7726-7734. DOI: 10.1021/acs.est.5b00381
- Liu, P., Garrido, B., Oksman, K., and Mathew, A. P. (2016). "Adsorption isotherms and mechanisms of Cu(II) sorption onto TEMPO-mediated oxidized cellulose nanofibers," *RSC Adv.* 6(109), 107759-107767. DOI: 10.1039/c6ra22397d
- Low, K. S., Lee, C. K., and Mak, S. M. (2004). "Sorption of copper and lead by citric acid modified wood," *Wood Sci. Technol.* 38(8), 629-640. DOI: 10.1007/s00226-003-0201-9
- Luo, X., Liu, L., Deng, F., and Luo, S. L. (2013). "Novel ion-imprinted polymer using crown ether as a functional monomer for selective removal of Pb(II) ions in real environmental water samples," *J. Mater. Chem. A* 1(28), 8280-8286. DOI: 10.1039/c3ta11098b
- Luo, X., Lei, X., Cai, N., Xie, X., Xue, Y., and Yu, F. (2016). "Removal of heavy metal ions from water by magnetic cellulose-based beads with embedded chemically modified magnetite nanoparticles and activated carbon," *ACS Sustain. Chem. Eng.* 4(7), 3960-3969. DOI: 10.1021/acssuschemeng.6b00790
- Melone, F., Saladino, R., Lange, H., and Crestini, C. (2013). "Tannin structural elucidation and quantitative ³¹P NMR analysis. 1. Model compounds," *J. Agric. Food Chem.* 61(39), 9307-9315. DOI: 10.1021/jf401477c
- Podschun, J., Saake, B., and Lehnen, R., (2015). "Reactivity enhancement of organosolv lignin by phenolation for improved bio-based thermosets," *Eur. Polym. J.* 67, 1-11. DOI: 10.1016/j.eurpolymj.2015.03.029
- Satapathy, R., Wu, Y. H., and Lin, H. C. (2012). "Novel dithieno-benzo-imidazole-based Pb(II) sensors: substituent effects on sensitivity and reversibility," *Chem. Commun.* 48(45), 5668-5670. DOI: 10.1039/c2cc31131c
- She, D., Xu, F., Geng, Z., Sun, R., Jones, G. L., and Baird, M. S. (2010). "Physicochemical characterization of extracted lignin from sweet sorghum stem," *Ind. Crop. Prod.* 32(1), 21-28. DOI: 10.1016/j.indcrop.2010.02.008
- Tofighy, M. A., and Mohammadi T. (2011). "Adsorption of divalent heavy metal ions from water using carbon nanotube sheets," *J. Hazard. Mater.* 185(1), 140-147. DOI:10.1016/j.jhazmat.2010.09.008
- Vasic, M., Sljukic, B., Wildgoose, G. G., and Compton, R. G. (2012). "Adsorption of bismuth ions on graphite chemically modified with gallic acid," *Phys. Chem. Chem. Phys.* 14(28), 10027-10031. DOI: 10.1039/c2cp41030c
- Wang, L., Zhang, J., Zhao, R., Li, Y., Li, C., and Zhang, C. (2010). "Adsorption of Pb(II) on activated carbon prepared from *Polygonum orientale* Linn.: Kinetics, isotherms, pH, and ionic strength studies," *Bioresour. Technol.* 101(15), 5808-5814. DOI: 10.1016/j.biortech.2010.02.099
- Wang, Y., Ye, G., Chen, H., Hu, X., Niu, Z., and Ma, S. (2015). "Functionalized metal-organic framework as a new platform for efficient and selective removal of cadmium(II) from aqueous solution," *J. Mater. Chem. A* 3(29), 15292-15298. DOI: 10.1039/c5ta03201f

- Xin, J., Zhang, P., Wolcott, M. P., Zhang, X., and Zhang, J. (2014). "Partial depolymerization of enzymolysis lignin via mild hydrogenolysis over Raney nickel," *Bioresour. Technol.* 155, 422-426. DOI: 10.1016/j.biortech.2013.12.092
- Ye, J., Abiman, P., Crossley, A., Jones, J. H., Wildgoose, G. G., and Compton, R. G. (2010). "Building block syntheses of gallic acid monomers and tris-(*O*-gallyl)-gallic acid dendrimers chemically attached to graphite powder: A comparative study of their uptake of Al(III) ions," *Langmuir* 26(3), 1776-1785. DOI: 10.1021/la902497s
- Zhang, L., Han, B., Li, T., and Wang, E. (2011). "Label-free DNazyme-based fluorescing molecular switch for sensitive and selective detection of lead ions," *Chem. Commun.* 47(11), 3099-3101. DOI: 10.1039/c0cc04523c
- Zhu, F., Lu, Y., and Li, L. (2016). "Synthesis, adsorption kinetics and thermodynamics of ureido-functionalized Pb(II) surface imprinted polymers for selective removal of Pb(II) in wastewater," *RSC Adv.* 6(112), 111120-111128. DOI: 10.1039/c6ra18736f

Article submitted: December 15, 2016; Peer review completed: April 6, 2017; Revised version received: April 17, 2017; Accepted: April 18, 2017; Published: June 7, 2017.
DOI: 10.15376/biores.12.3.5343-5357